JOC The Journal of Organic Chemistry

Article

pubs.acs.org/joc

A Combined Experimental and Theoretical Approach to the Photogeneration of 5,6-Dihydropyrimidin-5-yl Radicals in Nonaqueous Media

Isabel Aparici-Espert,[†] Antonio Francés-Monerris,[‡] Gemma M. Rodríguez-Muñiz,[†] Daniel Roca-Sanjuán,[‡] Virginie Lhiaubet-Vallet,*[,†] and Miguel A. Miranda*[,†]

[†]Instituto Universitario Mixto de Tecnología Química UPV-CSIC, Universitat Politècnica de València, Avda de los Naranjos s/n, 46022 València, Spain

[‡]Instituto de Ciencia Molecular, Universitat de València, P.O. Box 22085, 46071 València, Spain

Supporting Information

ABSTRACT: The chemical fate of radical intermediates is relevant to understand the biological effects of radiation and to explain formation of DNA lesions. A direct approach to selectively generate the putative reactive intermediates is based on the irradiation of photolabile precursors. But, to date, radical formation and reactivity have only been studied in aqueous media, which do not completely mimic the microenvironment provided by the DNA structure and its complexes with proteins. Thus, it is also important to evaluate the photogeneration of nucleoside-based radicals in nonaqueous media. The attention here is focused on the independent generation of 5,6-dihydropyrimidin-5-yl radicals in organic solvent through the synthesis of new lipophilic *tert*-butyl ketone precursors. Formation of 5,6-dihydro-2′-deoxyuridin-5-yl and 5,6-dihydrothymidin-5-yl radicals has first been confirmed by using a new nitroxide-derived profluorescent radical trap. Further evidence has been obtained by nanosecond laser flash photolysis through detection of long-lived transients. Finally, the experimental data are corroborated by multiconfigurational *ab initio* CASPT2//CASSCF methodology.

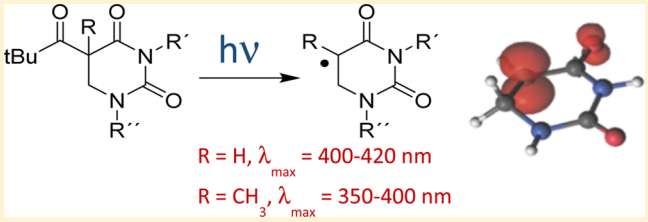

INTRODUCTION

Damage to DNA plays a significant role in the etiology and treatment of diseases. It often occurs through radical intermediates, which constitute the major family of reactive species generated in nucleic acids upon exposure to γ-radiolysis and Fenton conditions. Consequently, the chemical fate of these species is relevant to understand the biological effects of radiation and to explain formation of DNA lesions.[1−5] However, elucidating the chemistry of a specific radical is challenging because of the limitations imposed by the unselective nature of the involved processes. This problem has been tackled through independent generation of the putative reactive intermediates on isolated nucleosides as well as on synthetic oligonucleotides. In this context, modified nucleosides have been designed to achieve selective generation of the purported radicals upon appropriate activation.[2,6−9] Photolabile precursors have been very useful for studying the reactivity of sugar or nucleobase radicals involved in the formation of oxidatively generated damage in pyrimidine nucleosides. Light-absorbing moieties such as isopropyl or *tert*-butyl ketone, phenyl sulfide, or phenyl selenide have allowed the issue of the reactivity of carbon centered radicals at C5, C6, C1′, C2′, C3′, C4′, C5′ or at the thymine methyl group to be addressed.[6,7,10−20] Pulse radiolysis, laser flash photolysis, and electron paramagnetic resonance have been run on aqueous solutions of the pyrimidine or photolabile precursors,[21−23] and transient absorption spectra of the radicals of interest have been obtained by mathematical treatment of the whole signals usually corresponding to mixtures of several species.[23,24] From these results it has been concluded that 5,6-dihydrothymin-5-yl and related radicals show weak (ε ca. 1000 M^{-1} cm^{-1}) transient absorption spectra with broad maxima ranging from 380 to 460 nm[23,24] and lifetimes of hundreds of microseconds.[25]

With this background, the attention here is focused on the independent generation of 5,6-dihydropyrimidin-5-yl radicals in nonaqueous medium through the synthesis of new lipophilic *tert*-butyl ketone precursors. Photolysis of a *tert*-butyl ketone photolabile moiety at $\lambda > 300$ nm populates the nπ^* excited state, leading to radical formation through a Norrish type I photoreaction.[26] Indeed, this type of process has already been used to establish the chemical fate of thymidine and 2′-deoxyuridine C5 radicals inserted into synthetic oligonucleotides, characterized by strand breaks at the original site and at the adjacent 5′-nucleotide.[10−13,27] As stated above, the studies reported to date have been performed in aqueous media. In spite of the large amount of water in mammalian cells, the microenvironment provided by the DNA structure and its complexes with proteins such as histones may not be fully

Received: February 12, 2016
Published: April 18, 2016

DOI: 10.1021/acs.joc.6b00314
J. Org. Chem. 2016, 81, 4031−4038

Scheme 1. Synthetic Pathways To Obtain the C5-Radical Precursors Derived from Uridine and Thymidine[a]

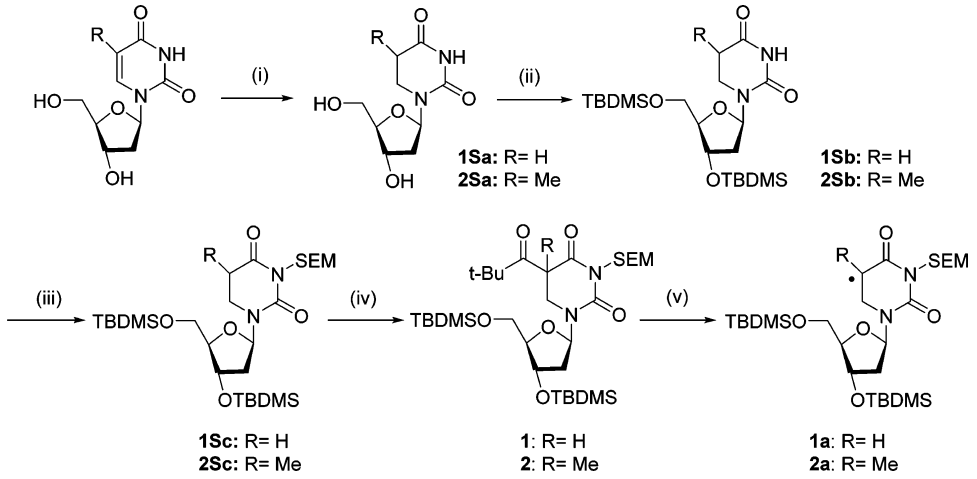

[a](i) H_2, Rh/Al_2O_3 in H_2O, rt; (ii) Imidazole, TBDMS-Cl in DMF, 0 °C → rt; (iii) iPr_2NEt, SEM-Cl in CH_2Cl_2, rt; (iv) LDA, Pivaloyl-Cl in THF, −78 °C; (v) $h\nu$.

reproduced by aqueous media, since the pyrimidine-derived radical would be embedded into the complex DNA/RNA system, which constitutes a heterogeneous and flexible environment. Nonaqueous media would also be of interest for the study of nucleic acid stability within the lipophilic surroundings supplied by vectors for gene delivery such as liposomes or polymers.[28,29] This is especially relevant for photochemical internalization based on an improved endolysosomal release by photoactivation of a sensitizer, which could originate DNA/RNA oxidative damage and loss of gene integrity.[30,31] In spite of its interest, information on nucleic acid reactivity in nonaqueous media is essentially lacking, except for the recently reported oxidation of DNA bases through one-electron transfer or hydroxyl radical attack.[32,33]

Hence, the spectroscopic study of lipophilic precursors of 5,6-dihydropyrimidin-5-yl radicals has now been addressed in acetonitrile as solvent. The main purpose of the work is to obtain transient absorption data of high value for subsequent time-resolved experiments in nonaqueous solutions, as well as to provide a new tool for future assessment of the possible modulating effect of organic solvents on the secondary reactions mediated by peroxyl radicals. The UV−vis absorption spectra of the precursors have been measured in acetonitrile to determine the functional excitation range required to trigger photodeprotection and to confirm carbon-centered radical formation via its trapping by a nitroxide-based profluorescent probe. Further evidence supporting generation of the 5,6-dihydropyrimidin-5-yl radical has been obtained by nanosecond laser flash photolysis. Finally, theoretical calculations based on the multiconfigurational complete-active-space second-order perturbation theory//complete-active-space self-consistent field (CASPT2//CASSCF) protocol corroborate the experimental results.

RESULTS AND DISCUSSION

The new C5-pivaloyl derivatives **1** and **2** were synthesized following procedures previously described in the literature for similar compounds (Scheme 1).[10,27,34] Briefly, the first step consisted of reduction of the C5−C6 double bond of uridine or thymidine by hydrogenation using Rh/Al_2O_3 as catalyst. Next, C5′and C3′ hydroxyl functions were protected with the *tert*-butyldimethylsilyl group (TBDMS), followed by protection of nitrogen in position 3 with *N*-2-trimethylsilylethyoxymethyl moiety (SEM) in order to increase the solubility in organic media. Finally, deprotonation of C5 by lithium diisopropylamide (LDA) and subsequent reaction with pivaloyl chloride led to the desired compounds.

The absorption spectra in acetonitrile showed a band centered at 285 or 315 nm for **1** and **2**, respectively (Figure S1 in Supporting Information). This absorption, assigned to the $n\pi^*$ singlet excited state of the pivaloyl moiety, is a relevant characteristic because it is linked to the possibility of performing selective UVA/UVB irradiation of the radical precursor when inserted in DNA.

The photofragmentation of precursors **1** and **2** was first investigated by using nitroxide-based fluorescent probes, a family of paramagnetic compounds that have been widely used to trap carbon-centered radicals.[35] Their application as fluorogenic probes has been reported for the study of numerous biological processes such as redox states detection, reactive oxygen species formation, etc.[35,36] This methodology, which can be employed with complex biological systems, takes advantage of an efficient intramolecular quenching of the fluorophore emission by the TEMPO moiety. Radical trapping by the nitroxide leads to a diamagnetic adduct (either alkoxyamine or N-oxide);[37,38] thereby the intramolecular quenching is suppressed, and the chromophore fluorescence is restored. Thus, a judicious choice of the fluorophore is key to obtain the photophysical and chemical properties that suit the desired analytical approach. Here, the selected fluorophore has to (i) exhibit a strong and unambiguous fluorescence emission; (ii) be efficiently quenched by TEMPO radical; (iii) be excited at long wavelengths, higher than 350 nm, where DNA does not absorb; and (iv) show little if any absorption in the 260−330 nm range, in order to not interfere with the absorbance of the *tert*-butyl ketone moiety.

Accordingly, 9-anthraceneacetic acid (**AAA**) was selected as an appropriate fluorophore because it fulfills the above requirements; specifically, it has an absorption spectrum that allows selective excitation at 365 nm and displays a clear structured fluorescence emission spectrum (Figure 1).[39] Preliminary steady-state and time-resolved emission measurements (Figure S2) were performed with **AAA** in the presence of 4-hydroxy-2,2,6,6-tetramethylpiperidine-1-oxyl (**4-OH-**

DOI: 10.1021/acs.joc.6b00314
J. Org. Chem. 2016, 81, 4031−4038

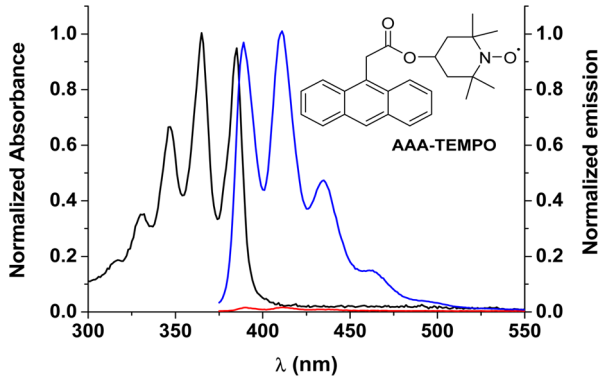

Figure 1. Absorption (black) spectrum and emission spectra of **AAA** (blue) and **AAA-TEMPO** (red) in acetonitrile, λ_{exc} = 365 nm.

TEMPO). In both experiments, an efficient quenching of the singlet excited state was observed with a bimolecular rate constant of ca. 10^{10} M^{-1} s^{-1}. Altogether, these data support the choice of **AAA** as the emissive species of the profluorescent probe.

Next, synthesis of the new **AAA-TEMPO** dyad was performed following a procedure given in the literature for similar compounds. In agreement with the expectations, the obtained probe exhibited only a very weak emission (Figure 1). Then, the ability of **AAA-TEMPO** to react with C-centered radicals was assessed by experiments in the presence of 2,2′-azobis(2-amidinopropane) dihydrochloride as a thermolabile radical initiator. An increase of the emission was observed when the azo compound was heated at 100 °C in the presence of the profluorescent probe (Figure S3). Thus, once established that **AAA-TEMPO** exhibits the typical behavior of nitroxide-based fluorescent probes, it was used to investigate the formation of the C5 centered radical by irradiation of **1** and **2**. When a deaerated acetonitrile solution of **1** or **2** (0.15 mM) was irradiated at 300 nm in the presence of **AAA-TEMPO** (0.032 mM), the anthracene emission increased steadily as a function of irradiation time (Figure 2). A control experiment performed under the same conditions but using a solution of uridine (or thymidine)/**AAA-TEMPO** allowed ruling out the occurrence of a H-abstraction process and supported trapping of the C5-centered radical. Irradiation of the probe alone in solution

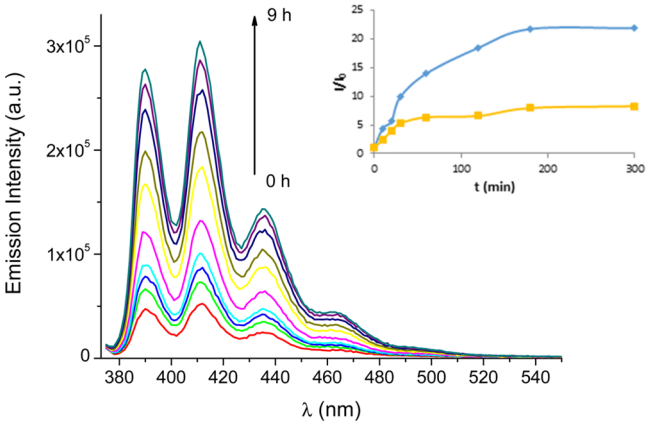

Figure 2. Emission spectra of N_2-bubbled acetonitrile solution of **AAA-TEMPO** in the presence of **1** (1:5), irradiated at λ = 300 nm. Inset: I/I_0 ratio as a function of irradiation time for **1** (blue) and **2** (orange); the values obtained for the probe alone has been subtracted.

revealed its photolability (Figure S4A); nonetheless, the generated fluorescence was consistently higher in the presence of **1** or **2** (Figure 2).

Steady-state photolysis was performed in order to confirm the formation of a covalent adduct between the profluorescent probe and the 5,6-dihydro-2′-deoxyuridine- or 5,6-dihydrothymidine-derived radicals. Analysis of the samples by UPLC-MS confirmed the formation of adducts with the exact mass m/z 978.5503 and 992.5699, corresponding to the molecular ion $[M + H]^+$ formula $C_{52}H_{84}N_3O_9Si_3$ and $C_{53}H_{86}N_3O_9Si_3$, respectively (Figure S5).

The next step was to characterize the photogenerated C5 radical by laser flash photolysis using 308 nm excitation. Thus, solutions of compounds **1** and **2** (1.24 and 2.23 mM, respectively) were prepared in acetonitrile and degassed under a nitrogen atmosphere. The transient absorption spectrum was registered 4 μs after the laser pulse in order to avoid the presence of misleading short-lived components such as the triplet excited state. Indeed, this delay was selected because of the long lifetime of the radicals of interest, which do not decay in a window of tens of microseconds.[24,25] Under these conditions, the transient absorption spectra were noisy, due to the low ε of the radical species; however, **1** exhibited a maximum at ca. 400−420 nm, whereas in the case of **2** blue-shifted maxima peaking at ca. 350−400 nm were observed (Figure S6). These data are in agreement with previous pulse radiolysis experiments; thus, the obtained transients were assigned to the C5-radicals.[23,24]

The experimental results were then compared with those obtained by theoretical calculations. For the sake of simplification, the studies were performed considering the chromophore structures **I**, **II**, **Ia**, and **IIa** (Figure 3). The multiconfigurational CASPT2//CASSCF protocol[40−43] was used in combination with the atomic natural orbital L-type (ANO-L) basis set contracted to C, N, O [4s3p1d]/H [2s1p],[44] as implemented in the MOLCAS 8 suite of programs,[45] to compute the vertical absorption energies and the oscillator strengths of the first nine excited states of the four species (details on the calculations can be found in the Supporting Information). This computational strategy has been successfully employed in the theoretical determination of the UV−vis spectra of the •OH adducts of the pyrimidine DNA/RNA nucleobases, which have related chemical structures.[46]

The theoretical results are compiled in Tables 1 and S2, where only the data for the three lowest-energy excited states are shown. Absorption of UVB light by compounds **I** and **II** at low energies corresponds to the population of the relatively dark S_1 state, which mainly involves the $n_{CO1} \rightarrow \pi_1^*$ excitation localized in the C=O bond of the pivaloyl fragment (see orbital labeling in Figure S7). Such an excited state was computed vertically at 4.11 eV (302 nm) and 3.93 eV (315 nm) for **I** and **II**, respectively. These theoretical predictions are in reasonable agreement with the experimental band maxima recorded at 4.35 eV (285 nm) for **1** and 3.93 eV (315 nm) for **2** (see Figure S1). Since the computed values were obtained for the molecules *in vacuo* while for the experimental measurements the compounds were dissolved in acetonitrile, the change of the module of the dipole moments between the excited and ground states was also analyzed; negligible solvatochromic shifts are expected for the low-lying excited states of **I** and **II**, according to the small $\Delta\mu$ values (see Tables 1 and S2). Although the agreement between theory and experiments for the absorption properties of the pivaloyl

DOI: 10.1021/acs.joc.6b00314
J. Org. Chem. 2016, 81, 4031−4038

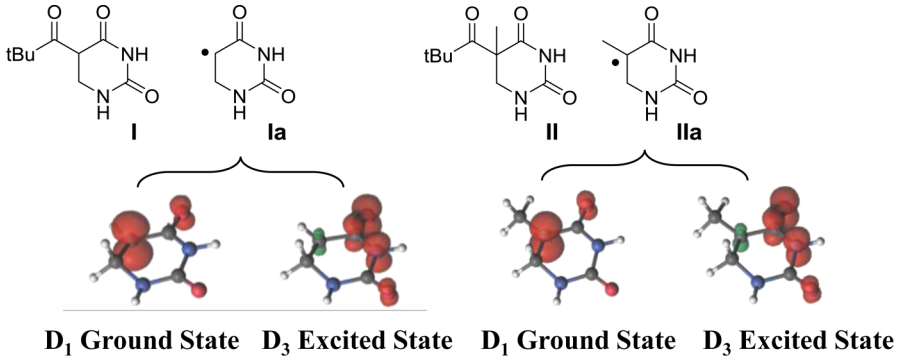

Figure 3. Structures of the models used in the theoretical calculations, **I** and **II** are singlet molecules, whereas **Ia** and **IIa** are doublet species. Representation of the difference between the α and β spin densities obtained from the computed CASSCF wave functions for the ground D_1 and excited D_3 states of **Ia** and **IIa** using an isovalue of 0.01; red and green colors indicate positive and negative spin densities, respectively.

Table 1. Nature of the Electronic Transition, CASPT2 Vertical Absorption Energies, Oscillator Strengths, and Module of the CASSCF Dipolar Moments Relative to the Ground State ($\Delta\mu = |\vec{\mu}|_{ES} - |\vec{\mu}|_{GS}$) for the Low-Lying Excited States of the Studied Species along with the Experimental Absorption Band Maxima Associated with the Corresponding Excited State[a]

compd	state	nature of the transition	vertical absorption energy/eV (nm)	oscillator strength (f) gs → es	$\Delta\mu$/D	experimental/eV (nm)
I	S_1	$n_{CO1} \rightarrow \pi_1^*$	4.11 (302)	0.00004	−0.02	4.35 (285)
II	S_1	$n_{CO1} \rightarrow \pi_1^*$	3.93 (315)	0.00004	−0.32	3.93 (315)
Ia	D_2	$n_{CO1} \rightarrow \pi_{SONO}$	2.57 (482)	0.00019	−1.42	
	D_3	$\pi_1 \rightarrow \pi_{SONO}$	3.21 (386)	0.02173	−2.84	2.95−3.10 (400−420)
	D_4	$\pi_2 \rightarrow \pi_{SONO}$	3.62 (342)	0.00290	5.82	
IIa	D_2	$n_{CO1} \rightarrow \pi_{SONO}$	2.74 (453)	0.00024	−1.20	
	D_3	$\pi_1 \rightarrow \pi_{SONO}$	3.35 (370)	0.02372	−3.04	3.54−3.10 (350−400)
	D_4	$\pi_2 \rightarrow \pi_{SONO}$	3.82 (325)	0.00235	5.06	

[a]Abbreviations: gs = ground state, es = excited state.

derivatives of uracil and thymine was not fully satisfactory, the trend was indeed coincident. Lower absorption energies were obtained for the compound with the methyl group. A parallel behavior has also been found when comparing the absorption spectra of the canonical nucleobases uracil and thymine.[47]

In the case of radical **Ia**, three excited states (D_2, D_3, and D_4) were computed at the energy range between 2.5 and 4.0 eV (see Table 1). Taking into account the oscillator strength (f) associated with the $D_1 \rightarrow D_3$ transition, which is much higher than that of the D_2 and D_4 states, the D_3 state is predicted as being mainly responsible for the broad experimental band peaking at 2.95−3.10 eV (400−420 nm). The vertical absorption energy of the state, computed at 3.21 eV (386 nm), is in quite good agreement with the recorded absorption maximum. Regarding the solvent effects, negligible impact on the absorption energy of the bright D_3 state is expected on the basis of its relatively small $\Delta\mu$ value. The D_4 vertical absorption energy of 3.62 eV (342 nm), the f of the transition, and its estimated red shift pointed to a non-negligible contribution of the $D_1 \rightarrow D_4$ excitation to the broad band. Likewise, the D_2 excited state participates in the ∼450 nm region. The f associated with the $D_1 \rightarrow D_2$ transition is much lower than that of the $D_1 \rightarrow D_3$ one, which is in agreement with the lower absorbance recorded experimentally in this region. Changes in the localization of the unpaired electron after excitation were tracked by analyzing the spin densities of the ground and excited states (see Figure 3). The **Ia** species in the D_1 ground state has the unpaired electron in a π singly occupied natural orbital (SONO) mainly localized at the C5 atom (see orbitals in Figure S8). The excitation process implies a redistribution of the spin density over the molecule, changing the radical position to other parts of the molecular structure. Thereby, in the D_3 state, the unpaired electron is in the π_1 natural orbital (NO) that is now mainly localized over the OCN atoms, as shown in the spin-density representations displayed in Figure 3.

The UV−vis absorption properties of the radical **IIa** are also summarized in Table 1. No relevant differences in the electronic nature of the ground and excited states were found with respect to those of **Ia**. Nevertheless, as a consequence of the methyl group at the C5 position, the vertical absorption energies are somewhat higher than those of **Ia**. This blue shift of around 0.1−0.2 eV is also observed in the experiments.

■ CONCLUSION

In summary, photolytic generation of the lipophilic 5,6-dihydropyrimidin-5-yl radicals in an organic medium has been achieved starting from *tert*-butyl ketone precursors. These species have been trapped by TEMPO-based profluorescent probes, and their transient absorption spectra have been obtained by laser flash photolysis. The experimental data have been corroborated by multiconfigurational *ab initio* CASPT2//CASSCF methodology. The obtained precursors should be of interest to investigate the reactivity of the 5-yl radical in organic solvents and to check whether 5-hydroperoxy-5,6-dihydropyrimidines after reduction to the stable 5-hydroxy-5,6-dihydropyrimidines are detected in the presence of O_2. Furthermore, insertion into defined sequence oligonucleotides could allow studying the reactivity of peroxyl radicals, once generated, with vicinal bases.

DOI: 10.1021/acs.joc.6b00314
J. Org. Chem. 2016, 81, 4031−4038

EXPERIMENTAL SECTION

Characterization. The ^{1}H and ^{13}C NMR spectra were measured by a 300 MHz instrument; $CDCl_3$ and D_2O were used as solvents, and the signal corresponding to the solvent was taken as the reference: 7.26 and 4.79 ppm, respectively, for ^{1}H NMR and 77.2 ppm for chemical shift of $CDCl_3$ in ^{13}C NMR. Coupling constants are given in Hz. Exact mass values were determined by using a QTof spectrometer coupled with a liquid chromatography system with a conditioned autosampler at 10 °C. The separation was carried out on an UPLC BEH C18 column (50 mm × 2.1 mm i.d., 1.7 μm). The column temperature was kept at 40 °C. The ESI source was operated in positive ionization mode with the capillary voltage at 1.9 kV. The temperature of the source and desolvation was set at 80 and 400 °C, respectively. The cone and desolvation gas flows were 20 and 800 L h^{-1}, respectively. All data were collected in centroid mode. Leucine-enkephalin was used as the lock mass generating an $[M + H]^+$ ion (m/z 556.2771) at a concentration of 250 pg/mL and flow rate of 50 μL/min to ensure accuracy during the MS analysis. The analysis of the irradiation of **1** (or **2**) in the presence of **AAA-TEMPO** was achieved under the same ESI conditions. But, in this case an isocratic elution was performed using 90% acetonitrile and 10% water (both containing 0.01% formic acid) as the mobile phase during the first 15 min followed by a gradient to reach 100% of acetonitrile at 17 min. The flow was maintained at 0.5 mL/min, and the injection volume was 1 μL. The **AAA-TEMPO** probe was characterized by the single crystal X-ray technique at 100 K temperature.

Photophysical Instrumentation. All experiments were performed in a quartz cuvette with a 1 cm optical path. Steady-state fluorescence experiments were performed by means of a spectrofluorometer, equipped with a Xe lamp (75 W) and a monochromator covering the region 200−700 nm. The time-resolved fluorescence experiments were carried out with a spectrometer equipped with a pulsed LED (λ_{exc} 340 nm) as an excitation source; the residual excitation signal was filtered in emission by using a cutoff filter (50% transmission at 365 nm). For the laser flash photolysis (LFP) experiments, a pulsed excimer laser instrument with a Xe/HCl mixture was used for excitation at 308 nm. The single pulses were of ca. 17 ns duration, and the energy was <100 mJ per pulse. A xenon lamp was employed as the detecting light source. The LFP apparatus consisted of the pulsed laser, the Xe lamp, a monochromator, and a photomultiplier (PMT) system made up of a side-on PMT, housing, and a power supply. The output signal from the Tektronix oscilloscope was transferred to a personal computer for study. All the experiments are performed under a N_2 atmosphere. A system including a Xe lamp (150 W) equipped with a monochromator was employed for steady-state monochromatic irradiation. The excitation wavelength was fixed at 300 nm, and the samples were irradiated for 5 h.

General Procedures for Synthesis of 1 and 2. *2′-Deoxy-5,6-dihydrouridine (**1Sa**).* Synthesis was performed following the method described by Greenberg et al.;[10] 0.25 g of the Rh/Al_2O_3 catalyst was added to 5 g of 2′-deoxyuridine in 50 mL of water under 30 bar of H_2. After purification, 4.4 g (96%) of **1Sa** was obtained as a colorless oil. ^{1}H NMR (300 MHz, D_2O) δ 6.26 (t, J = 7 Hz, 1H), 4.37 (m, 1H), 3.91 (m, 1H), 3.75 (m, 2H), 3.55 (m, 2H), 2.74 (t, J = 6 Hz, 2H), 2.31 (m, 1H), 2.13 (m, 1H). ^{13}C NMR (75 MHz, D_2O) δ 173.8 (CO), 154.2 (CO), 85.2 (CH), 84.0 (CH), 70.8 (CH), 61.6 (CH_2), 35.7 (CH_2), 35.2 (CH_2), 30.0 (CH_2). HMRS (ESI-TOF) m/z $C_9H_{14}N_2O_5Na$ $[M + Na]^+$ Calcd for 253.0800; Found: 253.0799.

*5,6-Dihydrothymidine (**2Sa**).* Synthesis was performed following established methods;[10,48,49] 0.25 g of the Rh/Al_2O_3 catalyst were added to 5 g of thymidine in 50 mL of water under 30 bar of H_2. After purification, 4.3 g (85%) of **2Sa** was obtained as a colorless oil. ^{1}H NMR (300 MHz, D_2O) δ 6.27 (t, J = 6 Hz, 1H), 4.35 (m, 1H), 3.88 (m, 1H), 3.71 (m, 2H), 3.56 (dd, J = 12.9, 5.6 Hz, 1H), 3.25 (m, 1H), 2.83 (m, 1H), 2.30 (m, 1H), 2.14 (m, 1H), 1.21 (d, J = 7.1 Hz, 3H). ^{13}C NMR (75 MHz, D_2O) δ 176.7 (CO), 154.3 (CO), 85.1 (CH), 83.8 (CH), 70.8 (CH), 61.6 (CH_2), 42.0 (CH_2), 35.4 (CH_2), 34.6 (CH), 12.1 (CH_3). HMRS (ESI-TOF) m/z $[M + H]^+$ Calcd for $C_{10}H_{17}N_2O_5$: 245.1137; Found: 245.1131.

*2′-Deoxy-3′,5′-bis-O-[(tert-butyl)dimethylsilyl]-5,6-dihydrouridine (**1Sb**).* 4.4 g (0.021 mol) of **1Sa**, 8.55 g (0.126 mol) of imidazole, and 11.4 g (0.076 mol) of *tert*-butyldimethylsilyl chloride were diluted in 35 mL of dimethylformamide at 0 °C. The mixture was allowed to reach room temperature and stirred overnight. Then, 250 mL of water were added, and extraction was performed with diethyl ether. The aqueous phase was further washed with diethyl ether (3 × 180 mL). The combined organic phases were mixed, washed with brine, dried with $MgSO_4$, and evaporated to dryness under reduced pressure. Purification was performed by flash column chromatography using hexane/ethyl acetate, 6/1 (v/v), as eluent, and 7.2 g (76%) of **1Sb** were obtained as a white solid. ^{1}H NMR (300 MHz, $CDCl_3$) δ 7.62 (br s, 1H), 6.28 (t, J = 7.0 Hz, 1H), 4.36 (m, 1H), 3.77 (m, 1H), 3.71 (m, 2H), 3.65 (m, 1H), 3.31 (m, 1H), 2.59 (m, 2H), 2.01 (m, 2H), 0.89 (m, 18H), 0.06 (m, 12H). ^{13}C NMR (75 MHz, $CDCl_3$) δ 169.9 (CO), 152.2 (CO), 86.5 (CH), 84.0 (CH), 72.1 (CH), 63.0 (CH_2), 37.8 (CH_2), 35.4 (CH_2), 31.3 (CH_2), 26.0 ($3CH_3$), 25.9 ($3CH_3$), 18.4 (C), 18.1 (C), −4.5 (CH_3), −4.7 (CH_3), −5.3 (CH_3), −5.4 (CH_3). HMRS (ESI-TOF) m/z $[M+ Na]^+$ Calcd for $C_{21}H_{42}N_2O_5Si_2Na$: 481.2530; Found: 481.2531.

*3′,5′-Bis-O-[(tert-butyl)dimethylsilyl]-5,6-dihydrothymidine (**2Sb**).* 4.3 g (0.018 mol) of **2Sa**, 7.2 g (0.106 mol) of imidazole, and 9.5 g (0.063 mol) of *tert*-butyldimethylsilyl chloride were diluted in 30 mL of dimethylformamide at 0 °C. The mixture was allowed getting to room temperature and stirred overnight. After addition of 250 mL of water and extraction with diethyl ether, the aqueous phase was further washed with diethyl ether (3 × 180 mL). The combined organic phases were mixed, washed with brine, dried with $MgSO_4$, and evaporated under reduced pressure. Purification was performed by flash column chromatography using hexane/ethyl acetate, 6/1 (v/v), as eluent. Compound **2Sb** (6.2 g) was obtained in 75% yield as a white solid. ^{1}H NMR (300 MHz, $CDCl_3$) δ 7.44 (br s, 1H), 6.30 (t, J = 7 Hz, 1H), 4.36 (m, 1H), 3.80 (m, 1H), 3.71 (m, 2H), 3.37 (m, 1H), 3.27 (m, 1H), 2.61 (m, 1H), 1.98 (m, 2H), 1.25 (d, J = 9 Hz, 3H), 0.89 (s + s, 18H), 0.06 (br s, 12H). ^{13}C NMR (75 MHz, $CDCl_3$) δ 172.8 (CO), 152.5 (CO), 86.6 (CH), 83.8 (CH), 72.2 (CH), 63.1 (CH_2), 42.1 (CH_2), 38.1 (CH_2), 35.6 (CH), 26.0 ($3CH_3$), 25.9 ($3CH_3$), 18.5 (C), 18.1 (C), 13.2 (CH_3), −4.5 (CH_3), −4.7 (CH_3), −5.3 (CH_3), −5.4 (CH_3). HRMS (ESI-TOF) m/z $[M+ H]^+$ Calcd for $C_{22}H_{45}N_2O_5Si_2$: 473.2867; Found: 473.2862.

*2′-Deoxy-3′,5′-bis-O-[(tert-butyl)dimethylsilyl]-3-[[2-(trimethylsilyl)ethoxy]methyl]-5,6-dihydrouridine (**1Sc**).* A solution of **1Sb** (7.23g, 0.016 mol) in 11 mL of *N,N*-diisopropylethylamine was mixed with 4.2 mL (0.024 mol) of 2-(trimethylsilyl)ethoxymethyl chloride diluted in 10 mL of CH_2Cl_2, and the mixture was stirred overnight at room temperature. Then, CH_2Cl_2 and a saturated solution of $NaHCO_3$ were added, and the organic phase was extracted, dried with $MgSO_4$, and concentrated under reduced pressure. Purification was performed by flash column chromatography using 10:1 hexane/ethyl acetate (v/v) as eluent, and 5.3 g (57%) of **1Sc** were obtained as a colorless oil. ^{1}H NMR (300 MHz, $CDCl_3$) δ 6.32 (t, J = 7 Hz, 1H), 5.21 (m, 2H), 4.34 (m, 1H), 3.83−3.56 (m,6H), 3.25 (m, 1H), 2.68 (m, 2H), 1.99 (m, 2H), 0.95−0.88 (m, 20H), 0.05 (brs, 12H), −0.02 (brs, 9H). ^{13}C NMR (75 MHz, $CDCl_3$) δ 169.7(CO), 152.9 (CO), 86.4 (CH), 84.8(CH), 72.0 (CH), 69.9 (CH_2), 67.0 (CH_2), 63.0 (CH_2), 37.9 (CH_2), 34.3 (CH_2), 32.0 (CH_2), 25.9 ($3CH_3$), 25.8 ($3CH_3$), 18.4 (CH_2), 18.2 (2C), −1.3 ($3CH_3$), −4.5 (CH_3), −4.7 (CH_3), −5.4 (CH_3), −5.5 (CH_3). HMRS (ESI-TOF) m/z $[M+ Na]^+$ Calcd for $C_{27}H_{56}N_2O_6Si_3Na$: 611.3344; Found: 611.3326.

*3′,5′-Bis-O-[(tert-butyl)dimethylsilyl]-3-[[2-(trimethylsilyl)ethoxy]-methyl]-5,6-dihydrothymidine (**2Sc**).* A solution of **2Sb** (4.3 g, 0.0091 mol) in 16 mL of *N,N*-diisopropylethylamine was mixed with 3.5 mL (0.02 mol) of 2-(trimethylsilyl)ethoxymethyl chloride diluted in 10 mL of CH_2Cl_2, and the mixture was stirred overnight at room temperature. Then, CH_2Cl_2 and a saturated solution of $NaHCO_3$ were added, and the organic phase was extracted, dried with $MgSO_4$, and concentrated under reduced pressure. Purification was performed by flash column chromatography using 10:1 hexane/ethyl acetate (v/v) as eluent, and 4.2 g (53%) of **2Sc** were obtained as colorless oil. ^{1}H NMR (300 MHz, $CDCl_3$) δ 6.35 (t, J = 9 Hz, 1H), 5.20 (s, 2H), 4.35 (m,

DOI: 10.1021/acs.joc.6b00314
J. Org. Chem. 2016, 81, 4031−4038

1H), 3.79 (m, 1H), 3.70 (m, 2H), 3.61 (m, 2H), 3.29 (m, 2H), 2.66 (m, 1H), 1.95 (m, 2H), 1.25 (d, J = 9 Hz, 3H), 0.90 (m, 20H), 0.06 (brs, 12H), −0.01 (s, 9H). ^{13}C NMR (75 MHz, $CDCl_3$) δ 172.8 (CO), 153.1 (CO), 86.5 (CH), 84.5 (CH), 72.2 (CH), 69.9 (CH_2), 66.9 (CH_2), 63.1 (CH_2), 40.8 (CH_2), 38.1 (CH_2), 36.0 (CH), 26.0 ($3CH_3$), 25.9 ($3CH_3$), 18.5 (2C), 18.2 (CH_2), 13.6 (CH_3), −1.3 ($3CH_3$), −4.5 (CH_3), −4.7 (CH_3), −5.3 (CH_3), −5.4 (CH_3). HMRS (ESI-TOF) m/z [M + Na]$^+$ Calcd for $C_{28}H_{58}N_2O_6Si_3Na$: 625.3500; Found: 625.3484.

*2′-Deoxy-3′,5′-bis-O-[(tert-butyl)dimethylsilyl]-3-[[2-(trimethylsilyl)ethoxy]methyl]-5-(2,2-dimethyl-1-oxopropyl)-5,6-dihydrouridine (**1**).* The final compound **1** was obtained as a diastereomeric mixture following the methodology described in the literature by Greenberg et al. for related compounds.[27] Briefly, a solution of **1Sc** (0.1 g, 1.7 × 10^{-4} mol) in tetrahydrofuran was stirred during 30 min with 0.85 mL of 2 M LDA at 78 °C. Then, pivaloyl chloride (0.02 mL, 1.6 × 10^{-4} mol) was added dropwise, and the mixture was kept at this temperature for 30 min. The organic phase was extracted after addition of a saturated solution of NH_4Cl and ethyl acetate (3 × 75 mL), washed with brine, dried with $MgSO_4$, and evaporated to dryness under reduced pressure. The purification was performed by preparative liquid chromatography (PLC) using 5:1 hexane/acetate (v/v) as eluent to afford compound **1** as a yellowish oil (0.06 g, 53%). ^{1}H NMR (300 MHz, $CDCl_3$) δ 6.34 (dd, J = 9 Hz, J = 6 Hz, 1H), 5.28 (d, J = 9 Hz, 1H), 5.15 (d, J = 9 Hz, 1H), 4.31 (m, 1H), 4.17 (m, 1H), 3.82 (m, 1H), 3.67−3.57 (m, 5H), 3.47 (m, 1H), 1.93 (m, 2H), 1.25−1.21 (m, 9H), 0.89 (m, 20H), 0.07 to −0.01 (m, 21H).^{13}C NMR (75 MHz, $CDCl_3$) δ 209.1 (CO), 207.6 (CO), 168.1 (CO), 167.9 (CO), 152.7 (CO), 152.2 (CO), 86.8 (CH), 86.7 (CH), 85.1 (CH), 84.8 (CH), 77.4 (C), 72.7 (CH), 72.4 (CH), 70.0 (CH_2), 67.1 (CH_2), 67.0 (CH_2), 63.6 (CH_2), 63.3 (CH_2), 47.9 (CH), 47.7 (CH), 45.5 (C), 38.2 (CH_2), 37.6 (CH_2), 37.4 (CH_2), 26.0 ($3CH_3$), 25.9 ($3CH_3$), 25.7 ($3CH_3$), 18.4 (C), 18.1 (CH_2), −1.3 ($3CH_3$), −4.5 (CH_3), −4.7 (CH_3), −5.3 (CH_3), −5.4 (CH_3). HRMS (ESI-TOF) m/z [M + Na]$^+$ Calcd for $C_{32}H_{64}N_2O_7Si_3Na$: 695.3919; Found: 695.3903.

*3′,5′-Bis-O-[(tert-butyl)dimethylsilyl]-3-[[2-(trimethylsilyl)ethoxy]-methyl]-5-(2,2-dimethyl-1-oxopropyl)-5,6-dihydrothymidine (**2**).* The final compound **2** was obtained following the methodology described in the literature by Greenberg et al. for related compounds.[27] Briefly, a solution of **2Sc** (0.1 g, 1.7 × 10^{-4} mol) in tetrahydrofuran was stirred for 3 h with 0.83 mL of 2 M LDA at 78 °C. Then, pivaloyl chloride (0.02 mL, 1.6 × 10^{-4} mol) was added dropwise, and the mixture was kept at this temperature for 1 h 30 min, allowed to reach room temperature, and stirred for additional 3 h. The organic phase was extracted after addition of a saturated solution of $NaHCO_3$ and ethyl acetate (3 × 75 mL), washed with brine, dried with $MgSO_4$, and evaporated to dryness under reduced pressure. The purification was performed by preparative liquid chromatography (PLC) using 5:1 hexane/acetate (v/v) as eluent to afford compound **2** as a transparent oil (0.07 g, 61%). ^{1}H NMR (300 MHz, $CDCl_3$) δ 6.39 (t, J = 6 Hz, 1H), 4.93 (m, 2H), 4.33 (m, 1H), 3.94 (d, J = 12 Hz, 1H), 3.75−3.63 (m, 4H), 3.50 (t, J = 6 Hz, 2H), 2.09 (m, 1H), 1.89 (m, 1H), 1.49 (s, 3H), 1.30 (s, 9H), 0.89 (m, 20H), 0.06 (br s, 12H), −0.02 (s, 9H). ^{13}C NMR (75 MHz, $CDCl_3$) (corresponds to the enol ester 2′ resulting from 1,3 acyl shift inside the NMR tube) δ 174.6 (CO), 153.8 (CO), 134.3 (CO), 94.1 (C), 86.0 (CH), 84.4 (CH), 72.1 (CH), 71.2 (CH_2), 65.0 (CH_2), 63.0 (CH_2), 42.1 (CH_2), 39.2 (C), 36.2 (CH_2), 27.1 ($3CH_3$), 26.1 ($3CH_3$), 25.9 ($3CH_3$), 18.5 (C), 18.1 (C), 18.0 (CH_2), 12.8 (CH_3), −1.2 ($3CH_3$), −4.5 (CH_3), −4.7 (CH_3), −5.2 (CH_3), −5.4 (CH_3). HMRS (ESI-TOF) m/z [M + H]$^+$ Calcd for $C_{33}H_{67}N_2O_7Si_3$: 687.4256; Found: 687.4271.

*2,2,6,6-Tetramethyl-4-(9-anthracenylacetoxy)-piperidine-1-oxyl (**AAA-TEMPO**).* The profluorescent probe **AAA-TEMPO** was obtained by esterification of 2-(anthracen-9-yl)acetic acid with 4-hydroxy-TEMPO, adapting a methodology described by Scaiano et al.[50] Briefly, 2-(anthracen-9-yl)acetic acid (0.2 g, 8.5 × 10^{-4} mol),[51] dicyclohexylcarbodiimide (0.2 g, 9.3 × 10^{-4} mol), 4-hydroxy-TEMPO (0.16 g, 9.3 × 10^{-4} mol), and 4-DMAP (0.01 g, 8.5 × 10^{-5} mol) were diluted with 4 mL of CH_2Cl_2 at room temperature and stirred until the esterification was completed (6 h). The precipitated *N,N*-dicyclohexyl urea was filtered off, and the filtrate was washed with H_2O (3 × 30 mL), 5% acetic acid solution (3 × 5 mL), and once more with H_2O (3 × 50 mL), dried with $MgSO_4$, and evaporated to dryness. Purification was performed by flash column chromatography using hexane/ethyl acetate 4:1 (v/v) as eluent to afford **AAA-TEMPO** as a coral-colored crystalline solid (0.256 g, 75%). The presence of the nitroxide prevented the characterization by NMR spectroscopy; thus, this compound was characterized by X-ray (CCDC 1444537; see Supporting Information).

Experimental Details of Fluorescence Studies. *Intermolecular Quenching of **AAA** by **4-OH-TEMPO**.* A solution of 2-(anthracen-9-yl) acetic acid **AAA** in acetonitrile (2.6 × 10^{-5} M) was prepared in a cuvette. On the other hand, a stock solution of **4-OH-TEMPO** (0.1 M) was prepared, so it was only necessary to add microliter volumes to the sample cell to obtain an appropriate concentration of the quencher. Quenching experiments were performed using an excitation wavelength λ_{exc} of 365 and 375 nm for steady-state and time-resolved studies, respectively. The rate constants for the reaction of **AAA** with **4-OH-TEMPO** were obtained from the Stern−Volmer plots[52] following eq 1 or 2 for steady-state and time-resolved measurements, respectively.

$$I_0/I = 1 + K_{SV} \times [\text{4-OH-TEMPO}] = 1 + k_q \times \tau_0 \times [\text{4-OH-TEMPO}] \quad (1)$$

where I_0 is the fluorescence intensity of **AAA** in the absence of quencher, I is the emission intensity after addition of a quencher concentration [**4-OH-TEMPO**] in molar, and K_{SV} is the Stern−Volmer constant (M^{-1}). A value of 109.4 M^{-1} was obtained for K_{SV} (Figure S2A).

$$1/\tau = 1/\tau_0 + k_q \times [\text{4-OH-TEMPO}] \quad (2)$$

where τ is the lifetime after addition of a quencher concentration [4-OH-TEMPO] and τ_0 is the lifetime for **AAA** in the absence of quencher. A τ_0 value of 4.7 ns was measured (Figure S2B), and a bimolecular quenching rate constant k_q of ca. 2 × 10^{10} M^{-1} s^{-1} was obtained from the Stern−Volmer plot (Figure S2B, inset). Moreover, it appears from eq 1 that k_q can be determined from K_{SV}. A k_q value of 2.3 × 10^{10} M^{-1} s^{-1} was thus obtained for the steady-state experiment, which rules out the occurrence of static quenching.

*Reactivity of **AAA-TEMPO** with 2,2′-Azobis(2-amidinopropane) Dihydrochloride.* An acetonitrile solution containing **AAA-TEMPO** (0.03 mM) and the radical initiator 2,2′-azobis(2-amidinopropane) dihydrochloride (0.03 mM) was heated at 100 °C for 8 h, and spectra were registered at different incubation times using an excitation wavelength of 365 nm (Figure S3).

*Reactivity of **AAA-TEMPO** with **1** and **2**.* Solutions containing **AAA-TEMPO** (0.03 mM) and **1** or **2** (0.15 mM) were irradiated monochromatically at 300 nm for up to 9 h. Emission spectra were registered at different irradiation times by exciting at 365 nm. A solution containing the probe alone was also monitored as a control experiment (Figure S4).

Experimental Details of Monochromatic Irradiation of AAA-TEMPO in the Presence of 1 or 2. Solutions containing **AAA-TEMPO** in the presence of **1** or **2** in a 1:5 ratio were irradiated monochromatically at 300 nm for 5 h. The solutions were concentrated and analyzed by UPLC-HRMS (Figure S5).

Computational Details. The theoretical spectra of the species **I**, **II**, **Ia**, and **IIa** have been computed by means of the complete-active-space second-order perturbation theory (CASPT2//CASSCF) protocol. This means that the ground-state geometries have been optimized at the CASSCF level, and then the vertical excitation energies have been calculated with the CASPT2 method at the CASSCF optimized geometry. The atomic natural orbital L-type (ANO-L) contracted to the C, N, O [4s3p1d]/H [2s1p] basis set has been used in all the calculations.

For the ground-state geometry optimizations, the multiconfigurational CASSCF wave functions have been built by including only the most relevant π molecular orbitals (MOs) in the active space. The following criterion has been used to choose the active orbitals: orbitals

DOI: 10.1021/acs.joc.6b00314
J. Org. Chem. 2016, 81, 4031−4038

with occupation numbers in the ground-state CASSCF calculations higher than 1.98 and lower than 0.02 are kept inactive and secondary, respectively, while natural orbitals with values in the range 1.98−0.02 are placed in the CAS space. The total number of active electrons and active MOs for each compound is summarized in Table S1. Thus, three π bonding MOs localized in the C═O bonds and the related π^* antibonding MOs have been included in the CAS for compounds **I** and **II**. On the other hand, two π MOs localized in the C═O bonds, the singly occupied natural orbital (SONO) mainly centered at the C5 position, and the two corresponding C═O π^* MOs have formed the active space of the **Ia** and **IIa** species. Only one root has been demanded in the CASSCF procedure for the ground-state optimizations.

For the vertical absorption energies, state-average (SA)-CASSCF calculations have been performed using 10 roots. All valence MOs have been included in the active space (see Table S1 and Figures S7 and S8). Calibration of the basis set, active space, and number of roots have been documented elsewhere.[46] All valence π and π^* MOs plus the lone pair orbitals of the oxygen atoms (n_{CO}) have been included in the active space (see Table S1 and Figures S7 and S8). The occupation numbers of the SA-CASSCF computations were used for this selection using the criterion described above. The dynamical electron correlation energies have been computed by means of perturbation theory with the CASPT2 method, using the SA-CASSCF wave function as reference. The zeroth-order Hamiltonian has been employed as originally implemented [ionization potential electron affinity (IPEA) parameter with a value of 0.0 au]. To minimize the effect of weak intruder states, the parameter of the imaginary level shift[53] has been fixed to 0.2 au.

Oscillator strengths (f) have been computed according to the formula

$$f = \frac{2}{3} E_{VA} \mathrm{TDM}^2$$

where E_{VA} refers to the CASPT2 vertical transition energy. The TDM stands for the transition dipole moment between the initial φ_1 and final φ_2 CASSCF wave functions, TDM = $\langle \varphi_1 | \vec{d} | \varphi_2 \rangle$, where $\vec{d}$ is the dipole moment operator.

All the calculations have been conducted with the MOLCAS 8 software package.

■ ASSOCIATED CONTENT

Supporting Information

The Supporting Information is available free of charge on the ACS Publications website at DOI: 10.1021/acs.joc.6b00314.

NMR spectra, X-ray, absorption and emission spectra, and computational details (PDF)

X-ray data for **AAA-TEMPO** (CIF)

■ AUTHOR INFORMATION

Corresponding Authors

*E-mail: lvirgini@itq.upv.es.

*E-mail: mmiranda@qim.upv.es.

Notes

The authors declare no competing financial interest.

■ ACKNOWLEDGMENTS

Spanish Government (CTQ2012-32621, CTQ2015-70164-P, CTQ2014-58624-P, RIRAAF RETICS RD12/0013/0009, Severo Ochoa program/SEV-2012-0267, María de Maetzu program/MDM-2015-0538, BES-2011-048326 and BES-2013-066566, JCI-2012-13431) and Generalitat Valenciana (Prometeo II/2013/005 and GV2015-057) are gratefully acknowledged. Dr. M. Luisa Marin is also acknowledged for her help during laser flash photolysis experiments.

■ REFERENCES

(1) Amato, N. J.; Wang, Y. *Chem. Res. Toxicol.* **2014**, *27*, 470.

(2) Rak, J.; Chomicz, L.; Wiczk, J.; Westphal, K.; Zdrowowicz, M.; Wityk, P.; Żyndul, M.; Makurat, S.; Golon, Ł. *J. Phys. Chem. B* **2015**, *119*, 8227.

(3) Dizdaroglu, M. *Int. J. Radiat. Biol.* **2014**, *90*, 446.

(4) von Sonntag, C. *Int. J. Radiat. Biol.* **2014**, *90*, 416.

(5) Cadet, J.; Douki, T.; Gasparutto, D.; Ravanat, J.-L.; Wagner, J. R. In *Encyclopedia of Radicals in Chemistry, Biology and Materials*; Chatgilialoglu, C., Studer, A., Eds.; John Wiley & Sons: Chichester, U.K., 2012; p 1319.

(6) Greenberg, M. M. *Chem. Res. Toxicol.* **1998**, *11*, 1235.

(7) Greenberg, M. M. *Org. Biomol. Chem.* **2007**, *5*, 18.

(8) Cadet, J.; Carell, T.; Cellai, L.; Chatgilialoglu, C.; Gimisis, T.; Miranda, M.; O'Neill, P.; Ravanat, J.-L.; Robert, M. *Chimia* **2008**, *62*, 742.

(9) Gimisis, T.; Chatgilialoglu, C. In *Encyclopedia of Radicals in Chemistry, Biology and Materials*; Chatgilialoglu, C., Studer, A., Eds.; John Wiley & Sons: Chichester, U.K., 2012; p 1345.

(10) Greenberg, M. M.; Barvian, M. R.; Cook, G. P.; Goodman, B. K.; Matray, T. J.; Tronche, C.; Venkatesan, H. *J. Am. Chem. Soc.* **1997**, *119*, 1828.

(11) Barvian, M. R.; Greenberg, M. M. *J. Org. Chem.* **1995**, *60*, 1916.

(12) Barvian, M. R.; Greenberg, M. M. *J. Am. Chem. Soc.* **1995**, *117*, 8291.

(13) Tallman, K. A.; Tronche, C.; Yoo, D. J.; Greenberg, M. M. *J. Am. Chem. Soc.* **1998**, *120*, 4903.

(14) Tronche, C.; Goodman, B. K.; Greenberg, M. M. *Chem. Biol.* **1998**, *5*, 263.

(15) Kroeger, K. M.; Hashimoto, M.; Kow, Y. W.; Greenberg, M. M. *Biochemistry* **2003**, *42*, 2449.

(16) Lahoud, G.; Fancher, J.; Grosu, S.; Cavanaugh, B.; Bryant-Friedrich, A. *Bioorg. Med. Chem.* **2006**, *14*, 2581.

(17) Manetto, A.; Georganakis, D.; Leondiadis, L.; Gimisis, T.; Mayer, P.; Carell, T.; Chatgilialoglu, C. *J. Org. Chem.* **2007**, *72*, 3659.

(18) Paul, R.; Greenberg, M. M. *J. Org. Chem.* **2014**, *79*, 10303.

(19) Paul, R.; Greenberg, M. M. *J. Am. Chem. Soc.* **2015**, *137*, 596.

(20) Shaik, R.; Ellis, M. W.; Starr, M. J.; Amato, N. J.; Bryant-Friedrich, A. C. *ChemBioChem* **2015**, *16*, 2379.

(21) Cullis, P. M.; McClymont, J. D.; Malone, M. E.; Mather, A. N.; Podmore, I. D.; Sweeney, M. C.; Symons, M. C. R. *J. Chem. Soc., Perkin Trans. 2* **1992**, 1695.

(22) Gregoli, S.; Cadet, J.; Shaw, A.; Voituriez, L.; Symons, M. C. R. *J. Chem. Soc., Perkin Trans. 2* **1985**, 1469.

(23) Deeble, D. J.; Das, S.; von Sonntag, C. *J. Phys. Chem.* **1985**, *89*, 5784.

(24) Ito, T.; Shinohara, H.; Hatta, H.; Nishimoto, S.-I.; Fujita, S.-I. *J. Phys. Chem. A* **1999**, *103*, 8413.

(25) Wójcik, A.; Naumov, S.; Marciniak, B.; Brede, O. *J. Phys. Chem. B* **2006**, *110*, 12738.

(26) Turro, N. J.; Ramamurthy, V.; Scaiano, J. C. *Modern Molecular Photochemistry of Organic Molecules*; University Science Books: Sausalito, CA, 2010.

(27) Resendiz, M. J. E.; Pottiboyina, V.; Sevilla, M. D.; Greenberg, M. M. *J. Am. Chem. Soc.* **2012**, *134*, 3917.

(28) Kay, M. A. *Nat. Rev. Genet.* **2011**, *12*, 316.

(29) Mintzer, M. A.; Simanek, E. E. *Chem. Rev.* **2009**, *109*, 259.

(30) Berg, K.; Berstad, M.; Prasmickaite, L.; Weyergang, A.; Selbo, P.; Hedfors, I.; Høgset, A. In *Nucleic Acid Transfection*; Bielke, W., Erbacher, C., Eds.; Springer: Berlin, Heidelberg, 2010; Vol. *296*, p 251.

(31) Rudiuk, S.; Franceschi-Messant, S.; Chouini-Lalanne, N.; Perez, E.; Rico-Lattes, I. *Photochem. Photobiol.* **2011**, *87*, 103.

(32) Capobianco, A.; Carotenuto, M.; Caruso, T.; Peluso, A. *Angew. Chem., Int. Ed.* **2009**, *48*, 9526.

(33) Rodríguez-Muñiz, G. M.; Marin, M. L.; Lhiaubet-Vallet, V.; Miranda, M. A. *Chem. - Eur. J.* **2012**, *18*, 8024.

(34) Kim, S. J.; Lester, C.; Begley, T. P. *J. Org. Chem.* **1995**, *60*, 6256.

(35) Blinco, J. P.; Fairfull-Smith, K. E.; Morrow, B. J.; Bottle, S. E. *Aust. J. Chem.* **2011**, *64*, 373.

DOI: 10.1021/acs.joc.6b00314
J. Org. Chem. 2016, 81, 4031−4038

(36) Kaur, A.; Kolanowski, J. L.; New, E. J. *Angew. Chem., Int. Ed.* **2016**, *55*, 1602.
(37) Cadet, J.; Berger, M.; Guttin-Lombard, M.; Bobenrietha, M. J. *Tetrahedron* **1979**, *35*, 2743.
(38) Berger, M.; Cadet, J.; Ulrich, J. *Can. J. Chem.* **1985**, *63*, 6.
(39) Alonso, R.; Yamaji, M.; Jiménez, M. C.; Miranda, M. A. *J. Phys. Chem. B* **2010**, *114*, 11363.
(40) Andersson, K.; Malmqvist, P. A.; Roos, B. O.; Sadlej, A. J.; Wolinski, K. *J. Phys. Chem.* **1990**, *94*, 5483.
(41) Andersson, K.; Malmqvist, P. Å.; Roos, B. O. *J. Chem. Phys.* **1992**, *96*, 1218.
(42) Roos, B. O.; Andersson, K.; Fülscher, M. P.; Malmqvist, P.-â.; Serrano-Andrés, L.; Pierloot, K.; Merchán, M. In *Advances in Chemical Physics*; Prigogine, I., Rice, S., Eds.; John Wiley & Sons: New York, 1996; p 219.
(43) Roca-Sanjuán, D.; Aquilante, F.; Lindh, R. *WIREs Comput. Mol. Sci.* **2012**, *2*, 585.
(44) Widmark, P.-O.; Malmqvist, P.-Å.; Roos, B. *Theor. Chim. Acta* **1990**, *77*, 291.
(45) Aquilante, F.; Autschbach, J.; Carlson, R. K.; Chibotaru, L. F.; Delcey, M. G.; De Vico, L.; Fdez. Galván, I.; Ferré, N.; Frutos, L. M.; Gagliardi, L.; Garavelli, M.; Giussani, A.; Hoyer, C. E.; Li Manni, G.; Lischka, H.; Ma, D.; Malmqvist, P. Å.; Müller, T.; Nenov, A.; Olivucci, M.; Pedersen, T. B.; Peng, D.; Plasser, F.; Pritchard, B.; Reiher, M.; Rivalta, I.; Schapiro, I.; Segarra-Martí, J.; Stenrup, M.; Truhlar, D. G.; Ungur, L.; Valentini, A.; Vancoillie, S.; Veryazov, V.; Vysotskiy, V. P.; Weingart, O.; Zapata, F.; Lindh, R. *J. Comput. Chem.* **2016**, *37*, 506.
(46) Francés-Monerris, A.; Merchán, M.; Roca-Sanjuán, D. *J. Chem. Phys.* **2013**, *139*, 071101.
(47) *Photoinduced Phenomena in Nucleic Acids I*; Barbatti, M., Borin, A. C., Ullrich, S., Eds.; Springer International Publishing: 2015.
(48) Kondo, Y.; Witkop, B. *J. Am. Chem. Soc.* **1968**, *90*, 764.
(49) Cadet, J.; Balland, A.; Berger, M. *Int. J. Radiat. Biol. Relat. Stud. Phys., Chem. Med.* **1981**, *39*, 119.
(50) Ballesteros, O. G.; Maretti, L.; Sastre, R.; Scaiano, J. C. *Macromolecules* **2001**, *34*, 6184.
(51) Shah, J. R.; Mosier, P. D.; Roth, B. L.; Kellogg, G. E.; Westkaemper, R. B. *Bioorg. Med. Chem.* **2009**, *17*, 6496.
(52) Stern, O.; Volmer, M. *Phys. Z.* **1919**, *20*, 183.
(53) Forsberg, N.; Malmqvist, P.-Å. *Chem. Phys. Lett.* **1997**, *274*, 196.

DOI: 10.1021/acs.joc.6b00314
J. Org. Chem. 2016, 81, 4031−4038